

Laboratory Studies of Stardust

ERNST ZINNER

Laboratory for Space Sciences and Physics Department, Washington University, St. Louis, Missouri 63130, USA

Introduction

Since the 1950s it has been established that carbon and all heavier elements are produced in stars and that these elements are produced in different stellar sources with very different isotopic ratios [e.g., 1]. Although many stellar sources must have contributed material to the solar system, it was believed that this material had been thoroughly mixed during solar system formation and resulted in very uniform isotopic ratios. As a consequence, signatures of individual stars had been completely obliterated and the solar system or “cosmic” abundances of elements and isotopes, although providing an important touchstone for stellar nucleosynthesis, represented only an average of distinct stellar sources. This situation has been dramatically changed with the discovery in 1987 that primitive meteorites contain tiny grains of pristine stardust. These grains condensed in the outflows of evolved stars and in supernova ejecta, survived interstellar travel and solar system formation, and are preserved in certain meteorites [2–5]. Their presolar, stellar origin is indicated by their isotopic compositions, which encompass a vast range and are completely different from that of the solar system. The grains can be located in and extracted from their meteoritic hosts and studied in detail in the laboratory. Because a given grain is a piece of a star, it can provide information on stellar evolution and nucleosynthesis, galactic chemical evolution, physical conditions in stellar atmospheres, dust processing in the interstellar medium, and condition during solar system formation. Since the discovery of the first presolar grains, their study has grown into a new kind of astronomy, complementing traditional astronomical observations. After a general overview and discussion of laboratory analysis techniques I will concentrate on issues of nucleosynthesis and topics of nuclear physics interests (sections 5–8). The reader interested in obtaining more detailed information is referred to some reviews on presolar grains [2–7].

Isolation of Presolar Grains

The first hints of the survival of presolar signatures in solar system materials came from isotopic anomalies, isotopic ratios different from those dominating the solar system, in hydrogen and the noble gases neon and xenon. However, these hints were largely ignored and it was not until the discovery of anomalies in oxygen, a major rock-forming element [8], that the idea of survival of presolar material in primitive meteorites was taken seriously. However, it turned out that the solids exhibiting isotopic anomalies in oxygen (and, as it was soon found, in many other elements) had formed in the solar system and only inherited presolar signatures from their precursors. It took more than a decade to find *bona fide* stardust that had condensed in stellar sources. This feat was achieved by Ed Anders and his colleagues at the University of Chicago by, as Anders put it, “burning down the haystack to find the needle” [9]. In this approach, chemical dissolution and physical separation techniques were used to track the carriers of anomalous, so-called exotic, noble gas components and led to the separation of presolar diamond [10], silicon carbide (SiC) [11,12], and graphite [13]. These phases are not only high-temperature phases that must have had a condensation origin, but are also chemically resistant and thus could be isolated by harsh chemical treatment.

Although these carbonaceous phases carried exotic noble gases, which aided in their discovery, and although almost all SiC and graphite grains are of stellar origin, the identification of presolar oxide grains is more difficult. The reason is that the solar system is oxygen-rich (i.e., has $O > C$), leading to the formation of oxygen-rich minerals from processed, that is, isotopically homogenized, material, which constitute a large background. Identification of presolar O-rich grains requires isotopic measurements of individual grains in the ion microprobe (see section 4). Separation of oxide phases such as corundum (Al_2O_3) and spinel ($MgAl_2O_4$) by chemical processing still helps, because the fraction of presolar grains among these phases is much higher (1–2%) [14,15] than among silicates, where

only one grain out of 5,000 grains, and that only for grains smaller than 1 μm , is of presolar origin [16].

Types of Presolar Grains

In spite of the grains' low abundance, their small size, and the background of isotopically normal grains of solar-system origin, an ever increasing number of different types of presolar minerals have been identified. Table 1 lists presolar grain types, their abundances, sizes, stellar sources, as well as nucleosynthetic signatures carried by the grains. Nanodiamonds are the most abundant, but they are only ~ 2.5 nm in size, precluding analysis of individual grains. Their presolar nature rests on the fact that they carry anomalous Xe and Te, but their average C isotopic ratio is normal (i.e., solar). Thus it cannot be ruled out that only a fraction of the diamonds have a stellar origin.

All other grain types are large enough that they can be analyzed as single grains for their isotopic compositions. Although silicates have the second-highest abundances, they have been discovered only in the last couple of years

because of the overwhelming presence of isotopically normal silicates [16,17]. The abundance of oxides is also relatively high but only among sub- μm grain in the most primitive meteorites. Silicon carbide is the best studied grain type because almost pure SiC separates can be produced by chemical processing of meteorites, and because trace element concentrations are high enough so that many elements can be analyzed in addition to C and Si. Average grain sizes are less than 1 μm but grains up to 20 μm have been found. Figure 1 a shows an SEM image of an unusually large grain. Analysis in the ion microprobe has shown enormous ranges in the isotopic compositions of individual grains (Figure 2) and has led to the classification of different sub-types according to the C, N, and Si isotopic ratios of the grains [18]. Mainstream, Y, and Z grains most likely originated in C-rich Asymptotic Giant Branch (AGB) stars. Grains of type X come from supernovae, grains of type A+B probably from J stars and/or from post-AGB stars that have undergone a very late thermal pulse, and a few grains appear to have a nova origin. Silicon nitride grains are

Table 1. Presolar grain types.

Grain type	Abundance* ppm	Size μm	Stellar sources	Nucleosynthetic processes [#] exhibited by grains
Nanodiamonds	1400	0.002	SNe	r, p
Silicates in IDPs	~ 900	≤ 1	RGB and AGB	Core H
Silicates in meteorites	180	≤ 0.5	RGB and AGB	Core H, CBP
Oxides	110	0.15–2	RGB, AGB, SNe	Core H, CBP, HBB, Shell H, He, s
Mainstream SiC	14	0.3–20	AGB	Core H, Shell H, Shell He, s
SiC type A+B	0.25	0.5–5	J stars?	Shell He and H
SiC type X	0.15	0.3–5	SNe	H, He, O, e, s, n-burst
Graphite	1	1–20	SNe, AGB	H, He, O, e, s, n-burst; Core H and He
Nova grains (SiC, gr.)	0.001	~ 1	Novae	Ex H
Si nitride	0.002	≤ 1	SNe	He, O
TiC	~ 0.001	0.01–0.5	SNe, AGB	He, O, e

*Abundances (in parts per million) vary with meteorite type. Shown here are the maximum values.

[#]In low-to-intermediate-mass stars: Core H: Core H burning followed by first (and second) dredge-up. Shell H: Shell H burning during the RG and AGB phase. Shell He: He burning during thermal pulses of AGB phase followed by third dredge-up. CBP: Cool bottom processing. HBB: Hot bottom burning. s: s-process, neutron capture at low neutron density, followed by third dredge-up.

In supernovae: H, He, O: H, He and O burning in different stellar zones in the massive star before explosion. e: s-process taking place in several zones. e: equilibrium process, leading to the Fe-Ni core. n-burst: Neutron capture at intermediate neutron density. r: Neutron capture at high neutron density. p: p-process, photo disintegration and proton capture.

In novae: Ex H: Explosive H burning.

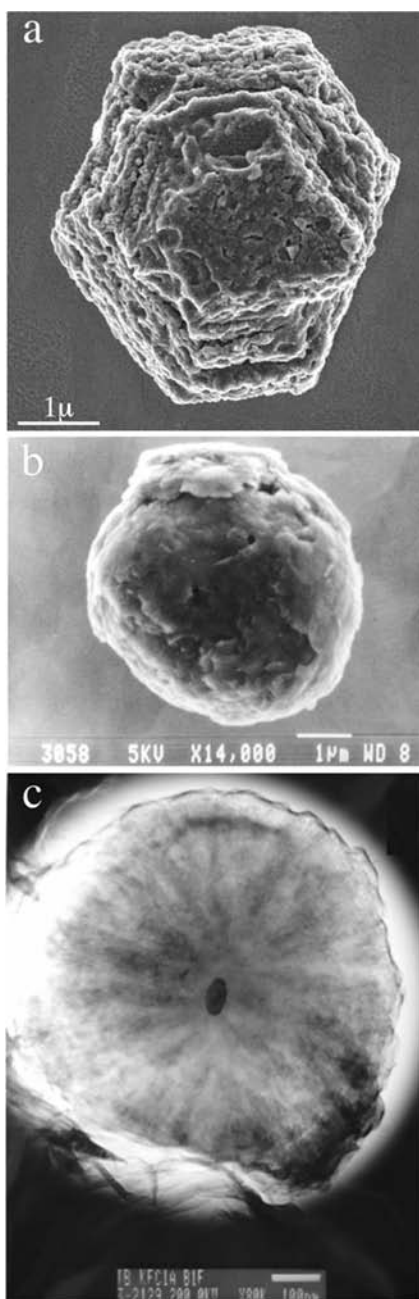


Figure 1. Secondary electron (a and b) and transmission electron (c) microscope images of presolar grains. (a) This large SiC grain shows euhedral features. (b) Graphite grain with smooth, shell-like surface (“onion type”). (c) TEM micrograph of a microtome slice of a presolar graphite grain. The TiC grain in the center of the graphite spherule apparently served as a condensation nucleus. Scale bars in a and b are 1 μm , in c 100 nm.

found in SiC-rich residues. They are extremely rare and have the isotopic signatures of SiC X grains, thus have a SN origin.

The separation of graphite is more complicated than that of SiC [19]. Most presolar graphite grains are larger than 1 μm (Figure 1b) and range up to 20 μm in size. They have been separated according to density [19]. Low-density grains have isotopic signatures that indicate a SN origin [20], whereas high-density grains seem to have an origin in C-rich AGB stars of low metallicity, that is, stars that were born with low abundances of “metals” (all elements heavier than He) [21]. Many graphite grains contain tiny sub-grains of titanium-, zirconium-, and molybdenum-rich carbides, cohenite (Fe_3C), kamacite (Fe-Ni) and elemental iron [22,23]. These grains must have condensed before the graphite and in some cases apparently acted as condensation nuclei (Figure 1c).

Analytical Techniques

Presolar grains have been analyzed for their size and morphology (SEM), internal structure (TEM), elemental (SIMS, Synchrotron XRS) and isotopic (SIMS, RIMS) compositions. Measurements of isotopic ratios are most important and by far most efforts have been devoted to them. Two basic types of isotopic analysis techniques have been applied, “bulk” analysis, the analysis of collections of large numbers of grains, and single grain analysis.

In spite of the low abundances of diamond, SiC and graphite in meteorites, chemical and physical separation provides essentially pure samples with enough grains for bulk analysis. Bulk analysis has been performed by Gas Mass Spectrometry for C, N, and the noble gases [24,25] and by Thermal Ionization Mass Spectrometry (TIMS) for the heavy elements Sr, Ba, Nd, Sm, and Dy [18]. Although only averages over many grains are obtained by these measurements, they make it possible to determine isotopic ratios of trace elements, which cannot be obtained on single grains. Measurements can be done on grain size and density separates, for gas MS by stepwise heating (pyrolysis) or combustion in an oxygen atmosphere.

Information on individual stars can be obtained by the analysis of single grains and correlations of isotopic ratios of several elements can serve to obtain the stellar history of a given grain. The technique of choice is Secondary Ion Mass Spectrometry (SIMS) with the ion microprobe. Single grain analysis revealed a tremendous range of isotopic ratios (see Figure 2). It also led to the identification of new grain types such as corundum and spinel [26] and silicon

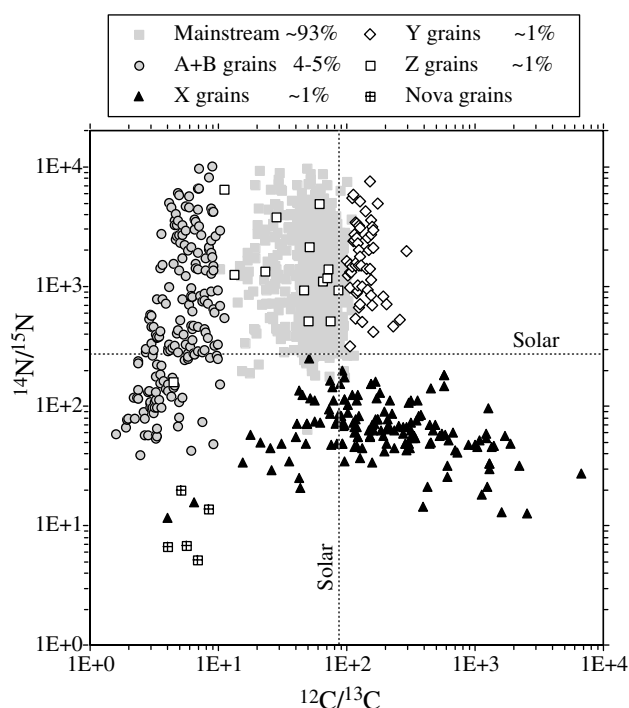


Figure 2. Nitrogen and carbon isotopic ratios of individual presolar SiC grains. Because rare grain types have been identified by special automatic imaging searches, the number of grains of different types do not correspond to their relative abundances in meteorites. These abundances are given in the legend. The dotted lines indicate the solar (terrestrial) isotopic ratios.

nitride [27], as well as of rare sub-populations of SiC grains. Although most isotopic measurements in the past have been made on $>1 \mu\text{m}$ grains, a new type of ion microprobe, the NanoSIMS (Figure 3) allows analysis of grains down to 100 nm in size. It was instrumental in the discovery of presolar silicates in interplanetary dust particles [17] and primitive meteorites [16]. Laser ablation and Resonant Ionization Mass Spectrometry (RIMS) has been applied to the isotopic analysis of the heavy elements Sr, Zr, Mo, Ru, and Ba in single presolar SiC and graphite grains [28–30]. The unique advantage of this technique is its high ionization efficiency and the fact that a chosen element can be ionized selectively at the exclusion of any isobaric interferences. Thus it is possible to measure Zr isotopes in the presence of Mo and vice versa. Single grain measurements of

He and Ne isotopes have been made by laser heating and gas MS [31].

s-process Nucleosynthesis

The agreement of the distribution of $^{12}\text{C}/^{13}\text{C}$ ratios found in carbon stars [32] with that in mainstream SiC grains indicates an origin in such stars. Further evidence is provided by the grains' N isotopic ratios and the presence of radioactive ^{26}Al (deduced from excesses in its daughter ^{26}Mg) and ^{22}Ne [24]. However, the most convincing evidence is obtained from the s-process patterns exhibited by all the heavy elements whose isotopic compositions have been measured to date (Figure 4). AGB stars have long been implicated as the main source of nuclei produced by the s-process, the slow capture of neutrons at neutron densities that are low enough that unstable isotopes can decay before another neutron is added [e.g., 33,34]. The evolution of the heavy elements thus progresses along the valley of stability. Two reactions provide neutrons in AGB stars: $^{13}\text{C}(\alpha,n)^{16}\text{O}$ and $^{22}\text{Ne}(\alpha,n)^{25}\text{Mg}$. The first occurs under radiative conditions in the intershell between the H- and He-burning shells between thermal pulses. It is responsible for most of the s-process production of the heavy elements.

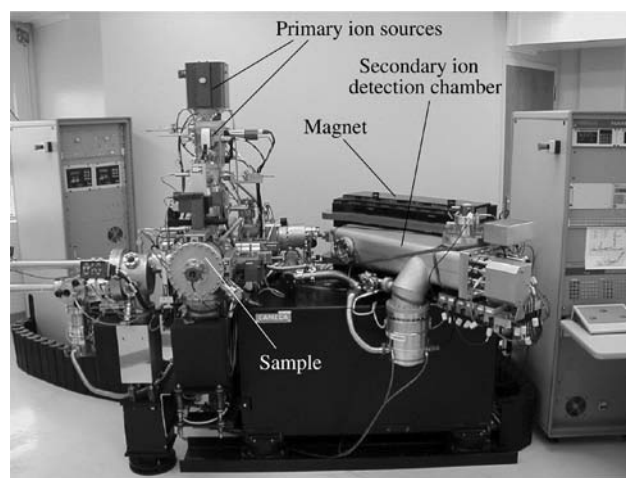


Figure 3. NanoSIMS, a new type of ion microprobe with high sensitivity and high spatial resolution. In this instrument a primary ion beam (Cs^+ or O^-) is focused onto the sample and by sputtering produces secondary ions. These ions are accelerated, separated according to their mass in a double-focusing magnetic mass spectrometer, and simultaneously detected in five different electron multipliers.

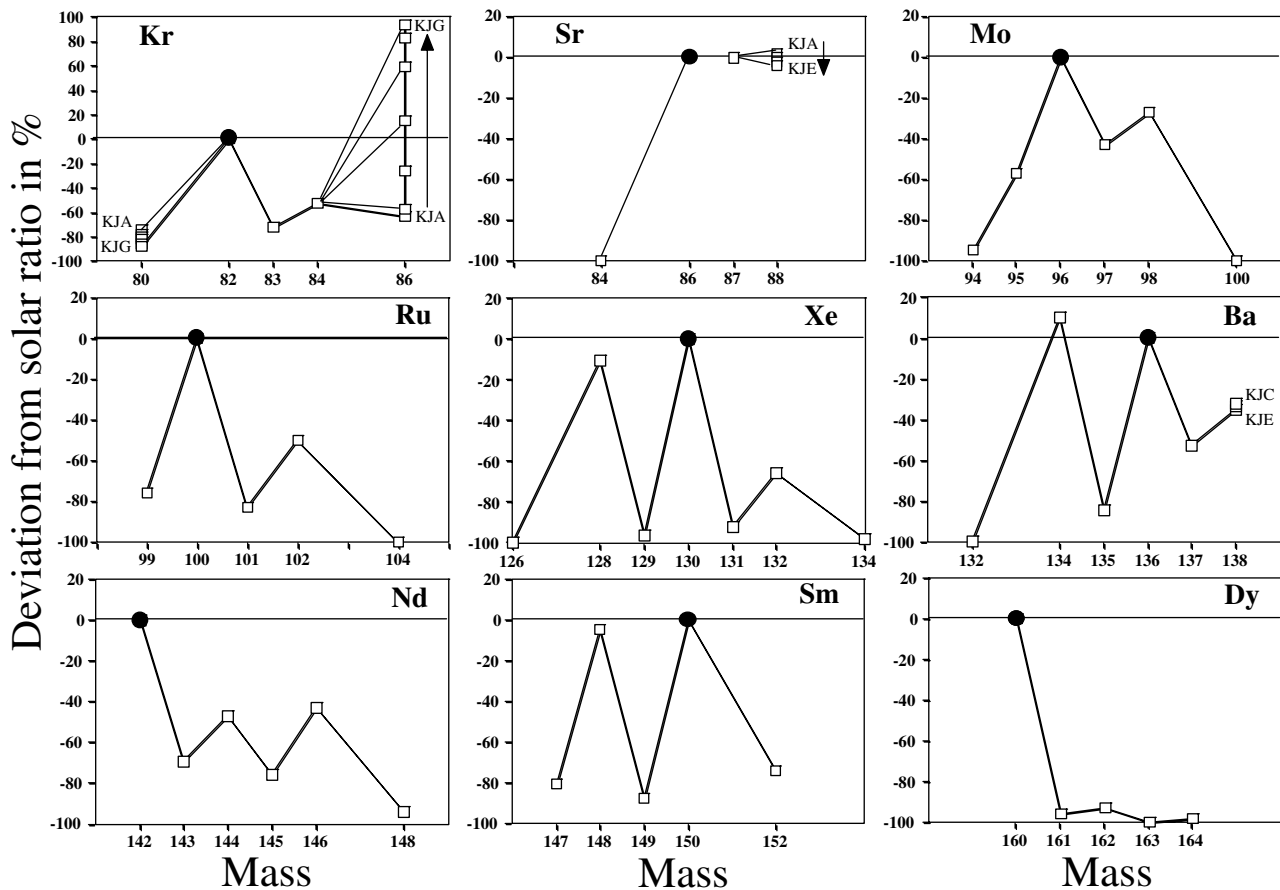


Figure 4. Isotopic patterns of heavy elements measured in presolar SiC grains. The isotopic ratios are relative to the reference isotope indicated by a filled circle and are plotted as deviations from the solar ratios in percentages. The zig-zag patterns seen are typical of production of the isotopes by the s-process, slow neutron capture, and in first order reflect the neutron capture cross-sections.

1

The second reaction occurs during the thermal pulses, lasts for a much shorter time, and results in much higher neutron densities [for details see Ref. (33)].

Figure 4 shows the isotopic patterns of heavy elements measured in bulk samples of SiC, which are dominated by mainstream grains. These patterns are characteristic of the s-process and for all elements except Dy agree very well with theoretical models of s-process nucleosynthesis in low-mass AGB stars [29,35]. The isotopic patterns allow the determination of different stellar parameters such as neutron exposure, temperature, and neutron density [18]. These parameters in turn depend on stellar mass and metallicity as well as on the neutron source. For example, the measured Ba patterns indicate a neutron exposure half of

that inferred for the solar system. Another example is provided by the abundance of ^{96}Zr , which is sensitive to neutron density because of the short half life (64 d) of ^{95}Zr . The low ^{96}Zr measured in individual grains indicates that the $^{22}\text{Ne}(\alpha, n)$ neutron source must have been weak, excluding intermediate-mass ($M > 3M_{\odot}$) AGB stars as parent stars of mainstream SiC grains [29].

2

One interesting consequence of isotopic measurements in presolar SiC grains was that some results motivated nuclear astrophysicists to determine neutron-capture cross-sections with high precision. Discrepancies between Ba and Nd isotopic patterns measured in presolar SiC and the results of model predictions led to the suggestion that the cross-section used in the theoretical calculations were

incorrect. This suspicion was confirmed by subsequent improved cross-section determinations that successfully resolved the discrepancies [36–38].

Grains from Supernovae

For a given presolar grain the stellar source is unknown and must be inferred from the grain's isotopic composition. From astronomical observations it was clear that RGB and AGB stars and supernovae were the most likely sources of the grains. A rare sub-type of SiC, the X grains have isotopic signatures that indicated a SN origin. These grains have large excesses of ^{28}Si relative to the heavier Si isotopes and most have ^{12}C and ^{15}N excesses (see Figure 2). Such signatures are predicted for different layers of core-collapse (Type II) supernovae [39,40]. The smoking gun for a SN origin of X grains was provided by the finding that they contain evidence for the presence of radioactive ^{44}Ti ($T_{1/2} = 60$ y) and ^{49}V ($T_{1/2} = 337$ d) at the time of their formation [41,42]. Both of these isotopes are only produced in supernovae, mostly in a layer that contains almost pure ^{28}Si . Evidence for a SN origin is also found in low-density graphite grains in the form of ^{15}N , ^{18}O , and ^{28}Si excesses as well as evidence for the initial presence of ^{41}Ca and ^{44}Ti [20]. Silicon carbide X grains exhibit a Mo isotopic pattern that is completely different from that found in mainstream grains (Figure 5). Interestingly, it is not the pattern expected for the r-process (rapid addition of neutrons at very high neutron densities) but has been successfully explained by a neutron-burst model at intermediate neutron densities [43]. A neutron burst is predicted to occur in a narrow O-rich zone of Type II supernovae and can account for the Mo pattern in X grains [40].

Although the overall isotopic signatures of grains are consistent with theoretical predictions, the grain data present fundamental problems. One is that these signatures are found in completely different layers of the supernovae: the high $^{26}\text{Al}/^{27}\text{Al}$ ratios found in X grains in the He/N zone[#], high $^{12}\text{C}/^{13}\text{C}$ and $^{18}\text{O}/^{16}\text{O}$ ratios in the underlying He/C zone, high $^{15}\text{N}/^{14}\text{N}$ ratios at the bottom of this zone, high neutron densities (n-burst) at the top of the underlying O/C zone, ^{28}Si , ^{44}Ti , and ^{49}V in the Si/S zone (^{44}Ti and ^{49}V also in the underlying Ni core). It is still unclear how these different layers can be mixed together to produce the isotopic signatures observed in the grains, in particular in view of

[#]The zones are named according to the two most abundant elements.

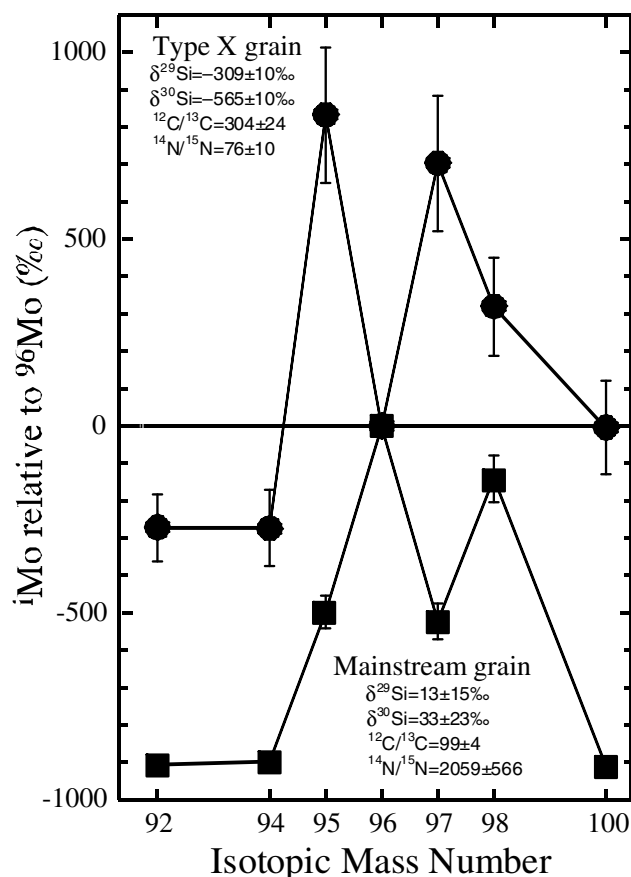


Figure 5. Isotopic patterns of Mo measured in a mainstream and a type X SiC grain. The plotted ratios are δ -values, deviations from the solar ratios relative to ^{96}Mo in permil (‰). Also given are the C, N, and Si isotopic ratios of the two grains. Figure courtesy of Andy Davis.

the fact that a huge layer consisting mostly of O lies between the C-rich layers and the Si/S layer. Another puzzle is why most of the SN grains identified so far are carbonaceous (SiC and graphite) and why only a handful of O-rich grains of a SN origin have been identified (Figure 6). Supernovae are predicted to contain far more O than C. Furthermore, theoretical models fail to predict in detail many isotopic ratios found SN grains [20]. Thus it is clear that the study of presolar grains provides new and fundamental challenges to nuclear astrophysicists.

Short-lived Radioisotopes

Many presolar grains contain evidence for the initial presence of short-lived, now extinct isotopes in the form of large

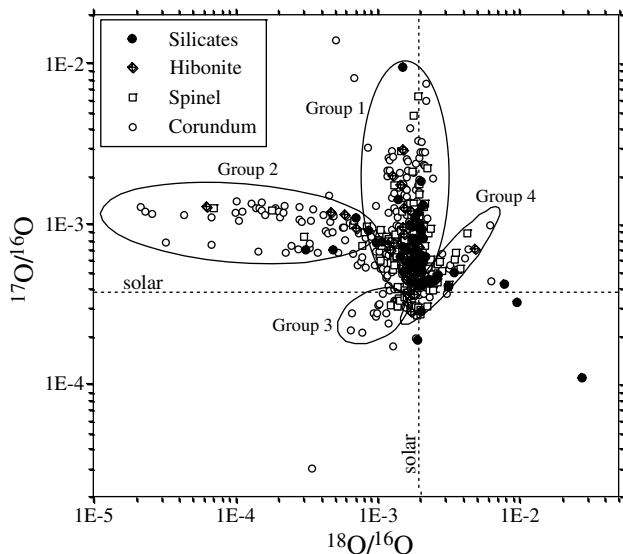


Figure 6. Oxygen isotopic ratios measured in individual O-rich presolar grains. The four groups defined by Nittler *et al.* [14] are indicated. The dotted lines indicate the solar (terrestrial) isotopic ratios.

excesses in the daughter isotopes of these radionuclides. In many cases these excesses are enormous so that there is little doubt that they are of radiogenic origin. I have already mentioned ^{44}Ti and ^{49}V . They are only produced in supernovae, both by α -rich freeze-out, ^{44}Ti also by Si burning, in the Si/S and Ni zones. Both are of general astrophysical interest for different reasons, ^{44}Ti because there is a chance that γ -rays from its decay can be detected in remnants of recent SN explosions, ^{49}V because the initial presence of this isotope with a half-life of only 337 days implies grain condensation in SN ejecta on a time scale of a couple of years. Because neutron capture in the He/C zone can also produce ^{49}Ti excesses [39,40], this signature by itself is no proof for initial ^{49}V . However, the correlation between ^{49}Ti excesses and the V/Ti ratio established its presence beyond any doubt [42].

Two other short-lived isotopes for which evidence was found in SN grains are ^{41}Ca ($T_{1/2} = 1.05 \times 10^5$ y) [44] and ^{26}Al ($T_{1/2} = 7.3 \times 10^5$ y) [for a summary see Ref. (3)]. In contrast to ^{44}Ti and ^{49}V , these two radionuclides are also produced in AGB stars and have, in fact, been detected in grains with an AGB origin. Inferred $^{41}\text{Ca}/^{40}\text{Ca}$ (from ^{41}K excesses) and $^{26}\text{Al}/^{27}\text{Al}$ (from ^{26}Mg excesses) ratios are much higher in SN grains than in grains from AGB stars. In SN grains the former range up to 1.6×10^{-2} , in agreement with theoretical predictions for n-capture production in the He/C,

C/O, and the O-rich zone of SNII [39,40]. The latter range up to 0.6 in X grains; the highest ratios are predicted for the He/N zone, where ^{26}Al is produced by proton capture on ^{25}Mg . $^{41}\text{Ca}/^{40}\text{Ca}$ measured in hibonite ($\text{CaAl}_6\text{O}_{19}$) grains from AGB stars [45] range up to 2×10^{-4} , in good agreement with theoretical predictions for n-capture production in the He shell. Inferred $^{26}\text{Al}/^{27}\text{Al}$ ratios in mainstream SiC grains (up to 2×10^{-3}) agree with predictions for production in the H shell of AGB stars [e.g., 46]. However, ratios in many oxide grain (corundum, spinel, hibonite, silicate) are much higher, as will be discussed in the next section.

A short-lived isotopes for which evidence has been only found in grains from AGB stars is ^{99}Tc ($T_{1/2} = 2.1 \times 10^5$ y). RIMS analysis of Ru isotopes in single mainstream SiC grains revealed s-process patterns with depletions in all Ru isotopes relative to s-process-only ^{100}Ru [30]. Whereas all measured ratios are in good agreement with AGB models, ^{99}Ru shows systematic excesses, which have been successfully explained by incorporation and decay of ^{99}Tc in the grains. It is fitting that a signature of this elements, whose presence in stars [47] was the first astronomical evidence for stellar nucleosynthesis, has now been found in stardust studied in the laboratory.

Evidence for Stellar Mixing

The isotopic analysis of presolar grains provides evidence for mixing processes in their stellar sources. I already mentioned the fact that SN grains carry isotopic signatures that have their origin in very different stellar zones. Their presence in individual grains implies mixing of these zones, although the details of these mixing processes are still not understood [20]. Another example where isotopic ratios measured in presolar grains indicate mixing in stars is provided by the O isotopic ratios of O-rich grains (Figure 6). The O isotopic compositions of Group 1 grains can be explained by core H burning and the first (and second) dredge-up whereby different $^{17}\text{O}/^{16}\text{O}$ ratios indicate different stellar masses [48]. Group 3 grains most likely come from low- and Group 4 grains from high-metallicity stars. However, the large ^{18}O depletions in Group 2 grains cannot be produced by standard models and an extra mixing process called cool bottom processing (CBP) has been proposed to explain them [49]. In this process, assumed to occur on the RGB and AGB, material from the convective envelope is believed to circulate to hot regions close to the H-burning shell where ^{18}O is destroyed by $^{18}\text{O}(p,\alpha)^{15}\text{N}$. Such extra mixing has also been invoked to explain low $^{12}\text{C}/^{13}\text{C}$ ratios and ^7Li and ^3He anomalies in RGB stars [50].

Additional evidence for CBP is given by the inferred $^{26}\text{Al}/^{27}\text{Al}$ ratios found in many oxide grains, which range up to 0.1

[14,45,51]. However, standard models of H shell burning in AGB stars result in ratios of only $\sim 2 \times 10^{-3}$ [46,52]. Consequently, CBP has also been invoked to account for the high $^{26}\text{Al}/^{27}\text{Al}$ ratios in oxide grains. In their model Nolle et al. [53] use two parameters to characterize CBP, the circulation rate, which mostly affects the $^{18}\text{O}/^{16}\text{O}$ ratio in the envelope, and the temperature reached by the circulated material, which mostly affects the $^{26}\text{Al}/^{27}\text{Al}$ ratio. Not all AGB stars experience CBP and one of the subjects of current research is which stars did and which ones did not. The parent stars of mainstream SiC grains apparently did not. Is it possible that CBP prevented O-rich stars from becoming carbon stars, so that evidence for effects of CBP on $^{26}\text{Al}/^{27}\text{Al}$ ratios are only seen in O-rich but not C-rich grains?

Conclusions

The study of presolar dust grains in the laboratory has become a new branch of astronomy. The grains provide information on isotopic ratios that could not be obtained from stars. Of special interest are results that do not agree with stellar models and thus trigger the introduction of new models (e.g., CBP), the measurement of cross sections (Ba, Nd), or the search for new processes not considered before (neutron burst). The field is vigorously expanding and technical advances are expected to yield new surprises.

References

1. G. Wallerstein et al., *Rev. Mod. Phys.* 69 (1997) 995.
2. E. Zinner, *Ann. Rev. Earth Planet. Sci.* 26 (1998) 147.
3. E. Zinner, in: *Meteorites, Planets, and Comets* (Ed. A. M. Davis), Vol. 1, *Treatise on Geochemistry* (Eds. H. D. Holland and K. K. Turekian), Elsevier-Pergamon, Oxford, (2004), pp. 17.
4. L. R. Nittler, *Earth & Planet. Sci. Lett.* 209 (2003) 259.
5. K. Lodders, S. Amari, *Chem. Erde* 65 (2005) 93.
6. T. J. Bernatowicz, E. Zinner (Eds.), *Astrophysical Implications of the Laboratory Study of Presolar Materials*, AIP, New York (1997).
7. D. D. Clayton, L. R. Nittler, *Annu. Rev. Astron. Astrophys.* 42 (2004) 39.
8. R. N. Clayton et al., *Science* 182 (1973) 485.
9. E. Anders, E. Zinner, *Meteoritics* 28 (1993) 490.
10. R. S. Lewis et al., *Nature* 326 (1987) 160.
11. T. Bernatowicz et al., *Nature* 330 (1987) 728.
12. M. Tang, E. Anders, *Geochim. Cosmochim. Acta* 52 (1988) 1235.
13. S. Amari et al., *Nature* 345 (1990) 238.
14. L. R. Nittler et al., *Astrophys. J.* 483 (1997) 475.
15. E. Zinner et al., *Geochim. Cosmochim. Acta* 67 (2003) 5083.
16. A. N. Nguyen, E. Zinner, *Science* 303 (2004) 1496.
17. S. Messenger et al., *Science* 300 (2003) 105.
18. P. Hoppe, U. Ott, in: *Astrophysical Implications of the Laboratory Study of Presolar Materials* (Eds. T. J. Bernatowicz and E. Zinner), AIP, New York, (1997), pp. 27.
19. S. Amari et al., *Geochim. Cosmochim. Acta* 58 (1994) 459.
20. C. Travaglio et al., *Astrophys. J.* 510 (1999) 325.
21. M. Jadhav et al., *New Astron. Rev.* 50 (2005) 591.
22. T. J. Bernatowicz et al., *Astrophys. J.* 472 (1996) 760.
23. T. K. Croat et al., *Geochim. Cosmochim. Acta* 67 (2003) 4705.
24. R. S. Lewis et al., *Geochim. Cosmochim. Acta* 58 (1994) 471.
25. S. Amari et al., *Geochim. Cosmochim. Acta* 59 (1995) 1411.
26. L. R. Nittler et al., *Nature* 370 (1994) 443.
27. L. R. Nittler et al., *Astrophys. J.* 453 (1995) L25.
28. G. K. Nicolussi et al., *Astrophys. J.* 504 (1998) 492.
29. M. Lugaro et al., *Astrophys. J.* 593 (2003) 486.
30. M. R. Savina et al., *Science* 303 (2004) 649.
31. R. H. Nichols, Jr. et al., in: *Advances in Analytical Geochemistry* (Eds. M. Hyman and M. Rowe), JAI Press Inc., (1995), pp. 119.
32. D. L. Lambert et al., *Astrophys. J. Suppl.* 62 (1986) 373.
33. M. Busso et al., *Ann. Rev. Astron. Astrophys.* 37 (1999) 239.
34. M. Lugaro et al., *Astrophys. J.* 586 (2003) 1305.
35. R. Gallino et al., in: *Astrophysical Implications of the Laboratory Study of Presolar Materials* (Eds. T. J. Bernatowicz and E. Zinner), AIP, New York, (1997), pp. 115.
36. K. H. Guber et al., *Phys. Rev. Lett.* 78 (1997) 2704.
37. P. E. Koehler et al., *Phys. Rev. C* 57 (1998) R1558.
38. K. Wisshak et al., *Nuclear Physics A* 621 (1997) 270c.
39. S. E. Woosley, T. A. Weaver, *Astrophys. J. Suppl.* 101 (1995) 181.
40. T. Rauscher et al., *Astrophys. J.* 576 (2002) 323.
41. L. R. Nittler et al., *Astrophys. J.* 462 (1996) L31.
42. P. Hoppe, A. Besmehn, *Astrophys. J.* 576 (2002) L69.
43. B. S. Meyer et al., *Astrophys. J.* 540 (2000) L49.
44. S. Amari et al., *Astrophys. J.* 470 (1996) L101.
45. L. R. Nittler et al., *Lunar & Planet. Sci.* XXXVI (2005) Abstract #2200.
46. N. Mowlavi, G. Meynet, *Astron. Astrophys.* 361 (2000) 959.
47. P. W. Merrill, *Astrophys. J.* 116 (1952) 21.
48. A. I. Boothroyd, I.-J. Sackmann, *Astrophys. J.* 510 (1999) 232.
49. G. J. Wasserburg et al., *Astrophys. J.* 447 (1995) L37.
50. C. Charbonnel, *Astrophys. J.* 453 (1995) L41.
51. E. Zinner et al., *Geochim. Cosmochim. Acta* 69 (2005) 4149.
52. A. I. Karakas, J. C. Lattanzio, *Publ. Astron. Soc. Australia* 20 (2003) 279.
53. K. M. Nolle et al., *Astrophys. J.* 582 (2003) 1036.



ERNST ZINNER